Ozone-Mediated Functionalization of Multi-Walled Carbon Nanotubes and Their Activities for Oxygen Reduction Reaction

Hengheng Xia [1,2], Yexin Zhang [2], Chunlin Chen [2], Wenlin Wu [2], Ken Yao [1,*], Jian Zhang [2,**]

[1] *Department of Chemistry, Shanghai University, Shanghai 200444, China*
[2] *Ningbo Institute of Materials Technology & Engineering, Chinese Academy of Sciences, Ningbo 315201, China*

ARTICLE INFO

Key words:
Multi-walled carbon nanotubes
Ozone oxidation
Functionalization
Oxygen reduction reaction

The functionalization of multi-walled carbon nanotubes (MWCNTs) by ozone treatment has been systematically investigated by using Raman spectroscopy, transmission electron microscopy (TEM), Fourier transform infrared spectroscopy (FTIR), X-ray photoelectron spectroscopy (XPS), organic elemental analysis (OEA) and Boehm titration. The results showed that the functionalization process occurred at defective sites (opened mouths, tube caps, debris, etc.) before opening caps and truncating walls, and finally the graphitic structure was deteriorated. The surface oxygen content first increased with the treatment time but kept at around 8.0 wt% after 5 h. The analysis of the distribution of oxygen-containing groups revealed that phenolic hydroxyl was gradually converted to carboxyl and lactone. The carboxyl was found to play a pivotal role to reduce the over-potentials when we used the functionalized MWCNTs as the catalyst for oxygen reduction reaction (ORR).

1. Introduction

Carbon nanotubes (CNTs) have attracted tremendous interests due to their wide applications in many fields such as catalysis, fuel cells, composite materials, electric devices, and so on[1,2]. However, the surface inertness of pristine CNTs leads to inferior dispersion in the matrix and weak interaction force at the interface, which essentially limits the large-scale applications of CNTs. The oxygen functionalities (ketonic carbonyl, lactone, phenolic hydroxyl, carboxyl, etc.) can endow CNTs with hydrophilicity to disperse in solvents and chemical reactivity for catalytic reactions[1,3]. Liquid-phase oxidation is often employed by refluxing or immersing CNTs in many strong corrosive reagents like HNO_3, H_2SO_4, H_2O_2 and $KMnO_4$[4], inducing the production of noxious gases and waste chemicals. On the contrary, gas-phase oxidation is much cleaner and more convenient[5]. Among all oxidative gases, ozone takes several unique advantages including easy accessibility from ozone generator, low capital cost and sustainability. Most importantly, the functionalization can be conducted even at room temperature due to the superior reactivity of ozone. Ultraviolet[6] and ultrasound[7] are capable to improve the efficiency of functionalization.

In order to control the distribution of oxygen functionalities on CNTs for a specific use, many researchers have made great efforts to clarify the reaction mechanism between CNTs and ozone. Lu et al. have predicted that ozone added to the double bonds of CNTs in an analogous way to that of alkenes and fullerenes through 1,3-dipolar cycloaddition reaction following the Criegee mechanism[8]. The primary ozonide as a proposed intermediate was unstable and might readily dissociate into carbonyl and epoxide[9,10]. Chiang et al. suggested that the intermediate was hydrotrioxide that could transform into C = O double bonds, peroxides or oxygen radicals before the formation of carboxyl and carbonyl[11]. The existence of peroxide intermediate was verified by Razumovskii et al. by using the electron spin resonance technique[10]. In contrast, Li et al.[7] revealed that the C = C double bonds were first converted to –C–OH and further oxidized to –C = O and O = C–OH, which was confirmed later by Vennerberg et al.[12].

Most recently, we found that the carboxylic groups were apt to play a determined role in oxygen reduction reaction (ORR), which was technically important for electrochemical devices and electrolysis processes[13]. We present here a systematic study on the ozone-mediated functionalization of MWCNTs by using various techniques including Raman spectroscopy, transmission electron microscopy (TEM), Fourier transform infrared spectroscopy (FTIR), X-ray photoelectron spectroscopy (XPS), organic elemental analysis (OEA) and Boehm titration. One mechanism will be proposed

* Corresponding author. Prof., Ph.D.; Tel.: +86 21 56388125; Fax: +86 21 56388125.
E-mail address: yao850618jp@yahoo.co.jp (K. Yao).
** Corresponding author. Prof., Ph.D.; Tel.: +86 574 87615956; Fax: +86 574 86669487.
E-mail address: jzhang@nimte.ac.cn (J. Zhang).

to describe both surface and bulk changes of MWCNTs in a flow of diluted ozone at room temperature. Additionally, the catalytic role of the carboxyl for ORR was further verified.

2. Experimental

The pristine MWCNTs (purity 97.5 wt.%, average diameter 12.9 nm, length 3–12 μm) were supplied by Shandong Dazhan Nanomaterials Co., Ltd., China, which were prepared by chemical vapor deposition. A flow of diluted ozone was generated under an ozone generator (WH-H-Y, Wohuan ozone Mechanical and Electrical Equipment Co., China) using pure oxygen as the gas source. NaOH, Na_2CO_3 and $NaHCO_3$ were analytical grade reagents (Sinopharm Chemical Reagent Co., Ltd.). 2 g pristine MWCNTs were placed in a quartz U-type reactor and treated in 0.5 L min^{-1} of diluted ozone (3.6 vol.% O_3) at room temperature for different reaction times ranging from 0.25 to 9 h.

The Raman spectra were collected with a Renishaw inVia-reflex spectrometer using back-scattered light from a 532 nm laser focused through a 50 × objective lens. TEM images were recorded by using a Tecnai F20 microscope (FEI) with an acceleration voltage of 200 kV. The infrared spectra were obtained by using Nicolet 6700 with samples dispersed and gently grinded the powder in KBr. The overall oxygen content of each sample was determined by an organic element analyzer (HORIBA EMGA-620W). XPS tests were performed on an AXIS Ultra DLD multifunctional X-ray photoelectron spectroscope with an Al $K\alpha$ radiation source under a vacuum of 10^{-9} Torr. The starting angel of the photoelectron was set at 90°, and the spectrum was calibrated with a C_{1s} spectrum of 284.6 eV.

Boehm titration is an effective method to quantify the concentrations of oxygen functionalities including carboxyl, phenolic hydroxyl and lactone. Briefly, the sample (~0.5 g) was stirred for 12 h in three different 25 mL 0.05 mol L^{-1} basic solutions of NaOH, Na_2CO_3 and $NaHCO_3$, respectively. After filtering, the filtrate was titrated by 0.05 mol L^{-1} hydrochloric acid with degassing of pure N_2 for complete CO_2 expulsion during the titration. The pH variety was recorded by a digital pH meter, and the endpoint was determined from the first derivative of the pH-volume plot. The concentrations of oxygen functionalities were calculated based on the following assumptions: NaOH can neutralize lactone, carboxyl and phenolic hydroxyl. Na_2CO_3 can neutralize both lactone and carboxyl, while $NaHCO_3$ could merely neutralize the carboxyl. The difference between the uptakes of the bases can be used to quantify a specific functionality.

All electrochemical tests were carried out with a CHI 760E electrochemistry workstation (Shanghai CH Instruments, China) and a conventional three-electrode test cell at 25°C. A glassy carbon disk coated with catalyst was used as the working electrode. The counter-electrode and reference-electrode were a graphitic rod and a 3 M Ag/AgCl, respectively. The glassy carbon disk was polished with 30 nm alumina powder, sonicated and rinsed with deionized water and ethanol before used. The homogeneous catalyst ink was prepared by ultrasonically dispersing the mixture of 1 mg catalyst, 400 μL H_2O, 50 μL acetone and 50 μL Nafion alcohol solution (DuPont, 5 wt% Nafion) for 15 min. 5 μL catalyst ink was subsequently pipetted out and spread on a 3 mm-diameter cleaned glassy carbon disk as the working electrode with the areal loading amount of 141.5 μg cm^{-2} MWCNTs. To evaluate the catalytic activity for ORR, the cyclic voltammetry tests were carried out in 0.1 mol L^{-1} KOH solution saturated with 20 sccm ultrapure O_2 at a scanning rate of 100 mV s^{-1}.

3. Results and Discussion

Raman spectroscopy is a common method to characterize the structure changes of carbon materials[14,15]. Fig. 1(a) presents the Raman spectra of pristine and treated MWCNTs, in which two prominent peaks centering at 1344 and 1575 cm^{-1} can be assigned to the defect-induced disorder (D) mode and graphite (G) mode, respectively. The D to G intensity ratio, e.g. $R = I_D/I_G$, could reflect the structural amorphization of MWCNTs. The dependencies of R value and weight loss on the treatment time are depicted in Fig. 1(b) and 1(c). The weight loss almost linearly increased with the treatment time, while the tendency of R value comprised three stages. In the initial 3 h, the R value slightly increased from 1.11 to 1.13, while the weight loss gradually approached to 10.7%. Then, a sharp rise in R value was observed at 5 h and the value reached 1.34, being 21% higher than that of the pristine sample, but the weight loss of MWCNTs gradually increased with the treatment time without any abrupt change. Finally, as the treatment time being extended to 9 h, the R value slowly went up from 1.34 to 1.38.

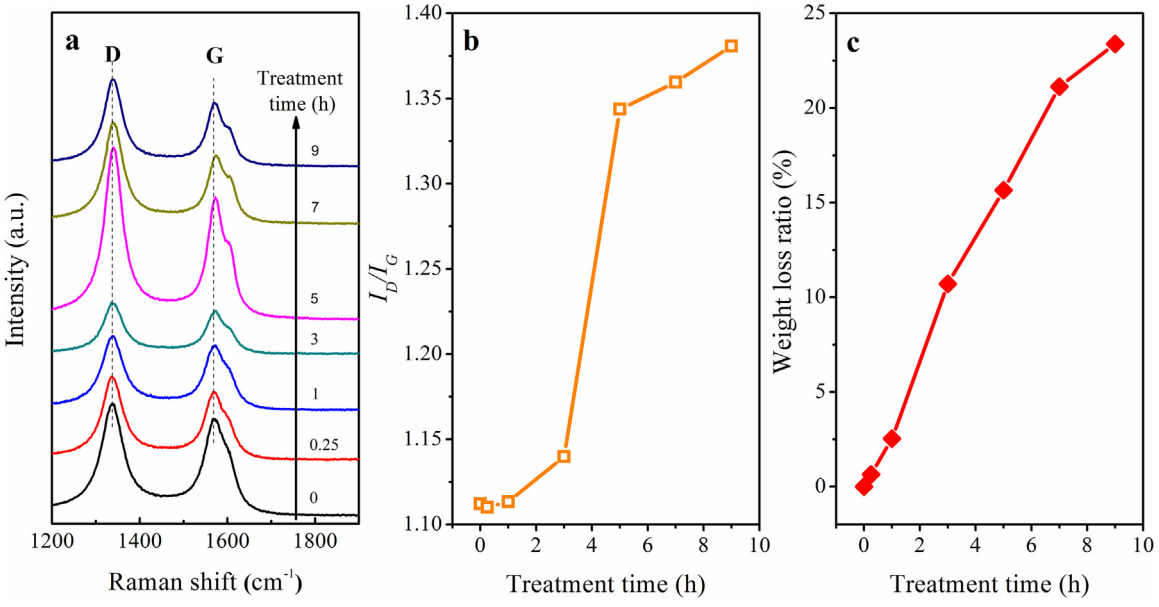

Fig. 1. (a) Raman spectra of pristine and treated MWCNTs; (b) the variation of I_D/I_G value; and (c) weight loss ratio with the ozone treatment time.

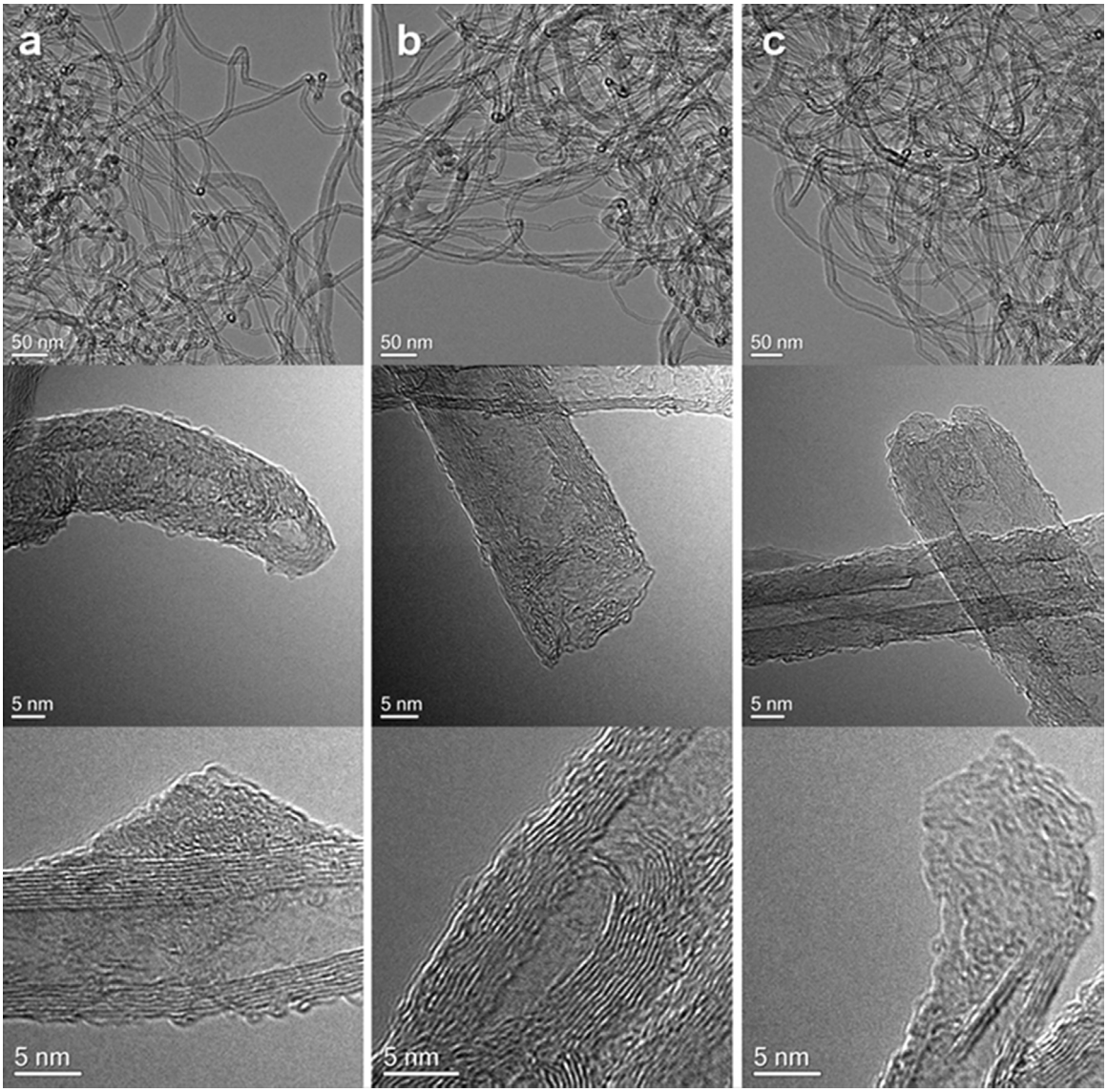

Fig. 2. Representative TEM images of pristine MWCNTs (a) and samples treated for 3 h (b) and 9 h (c).

To make clear the changes in structural and surface properties, we characterized all samples by TEM, FTIR, and XPS. Fig. 2 shows the representative TEM and high-resolution TEM images of pristine and treated MWCNTs. Before the contact with ozone, the pristine MWCNTs (Fig. 2(a)) possessed intact tube structure with closed caps, and with some residual amorphous carbons attaching to the outer walls. After being oxidized for 3 h, as displayed in Fig. 2(b), the amorphous species were burnt off. The outer walls of MWCNTs became clean and smooth with etched caps, while the inner walls were free of obvious change. With increasing the treatment time, the caps were thoroughly opened and the graphitic walls were etched to some extent (Fig. 2(c)). The nanotubes were truncated or shortened to result in a dramatic increase of *R* value (Fig. 1(b)).

Ozone treatment also introduced various oxygen functionalities on MWCNTs. The FTIR spectra of Fig. 3 indicated the presence of some oxygen functionalities such as carboxylic acids, ester and quinone[16]. The oxygen contents of all samples were determined by OEA and XPS as shown in Fig. 4(a). Note that XPS is a common surface technique to obtain the distribution of the surface oxygen (surf-O) species on the outer walls of MWCNTs, whereas OEA gives

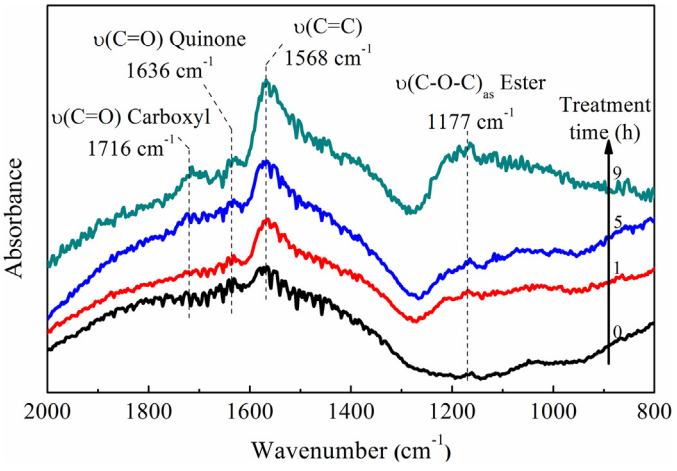

Fig. 3. FTIR spectra of MWCNTs samples with the treatment time.

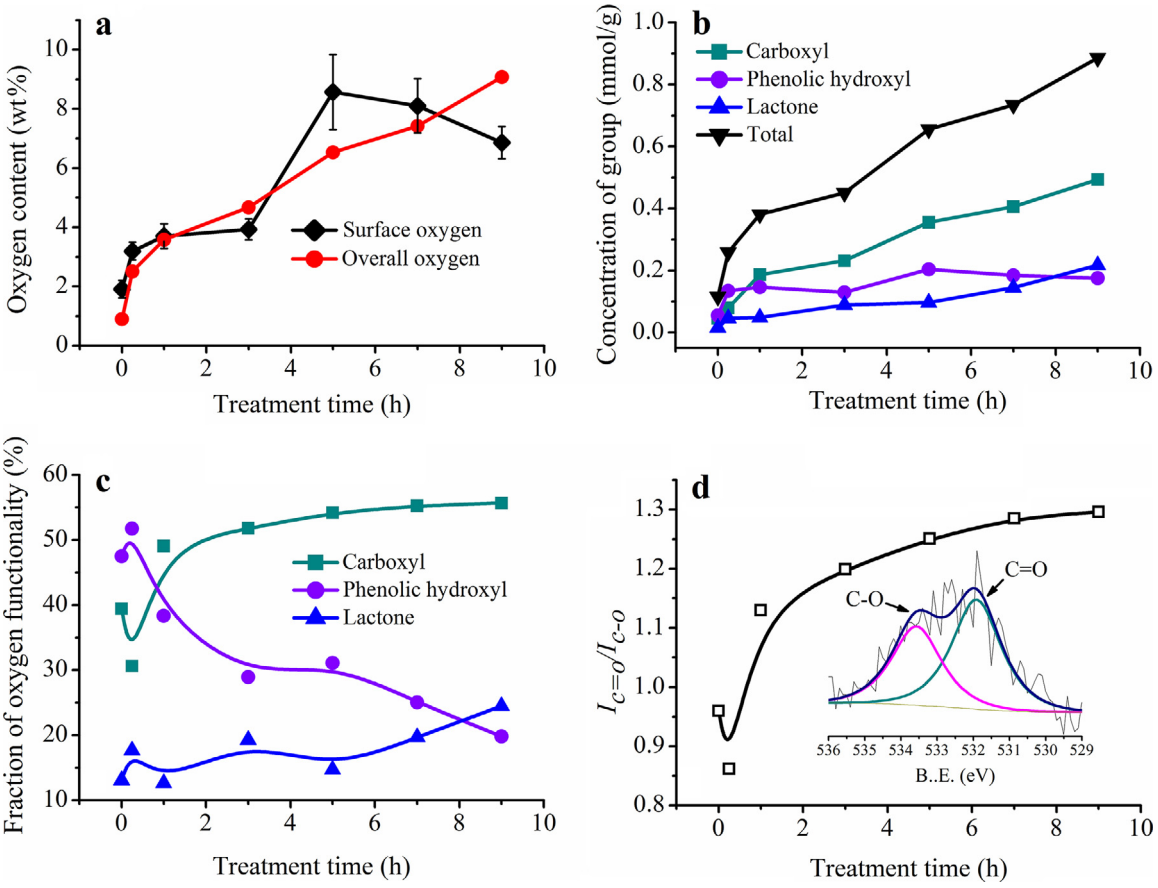

Fig. 4. (a) Oxygen contents determined by OEA and XPS; (b) Concentrations of oxygen functionalities determined by Boehm titration; (c) Fractions of oxygen functionalities determined by Boehm titration, and (d) $I_{C=O}/I_{C-O}$ derived from O_{1s} XPS peak as a function of treatment time. Inset (d): the deconvolution of O_{1s} peak of the MWCNTs after treated for 9 h.

the overall oxygen (over-O) content. Both surf-O and over-O got a sudden increase during the initial 0.25 h treatment and then the increase slowed down. Subsequently, the over-O content almost linearly approached to 9.08 wt% after treating for 9 h. Differently, the surf-O content increased sharply after 3 h treatment. But a decrease of surf-O content was observed after treating for 5 h. It was noted that the great increase of the surf-O content coincided exactly with the abrupt change of *R* value in Raman analysis (Fig. 1(b)), suggesting that the oxygen functionalization approached exactly with the oxidative etching. The concentrations of carboxyl, phenolic hydroxyl and lactone were quantified by Boehm titration (Fig. 4(b, c). To evaluate the possible disturbance of the residual metal catalyst particles contained in the CNTs framework, we first used ICP-OES to analyze the amount of metal ions in the titration solution. The maximum amount of Fe ions was below 2.0 μmol $gCNTs^{-1}$, giving a negligible influence on the calculation of the oxygen functional groups. The concentrations of carboxyl and lactone gradually increased with treatment time, while that of phenolic hydroxyl kept almost unchanged. However, the distributions of oxygen functionalities in Fig. 4(c) showed that the fraction of the phenolic hydroxyl significantly decreased, but that of the carboxyl increased with the treatment time. The phenolic hydroxyl was prevailing at the initial stage but subsequently declined to 19.8% at 9 h. While the proportion of the carboxyl showed an opposite tendency and finally reached 55.7%. This evidence suggested that the phenolic hydroxyl was most possibly oxidized into the carboxyl under the atmosphere of ozone, which could be further verified by the XPS analysis in Fig. 4(d). The insert pattern revealed that the O_{1s} spectrum could be deconvoluted into two species, being assigned to C = O and C–O components that centered at (531.8 ± 0.2) eV and (533.4 ± 0.2) eV, respectively[3]. The intensity ratio of C = O and C – O, $I_{C=O}/I_{C-O}$, was found to greatly increase at the initial period and gradually rise with the treatment time, coinciding with the result revealed by Boehm analysis (Fig. 4(c)). The oxidative conversion of the phenolic hydroxyl into carboxyl was also observed elsewhere[7,12,17].

Based on the above results, we proposed a three-stage mechanism of O_3-mediate functionalization of MWCNTs (Scheme 1). At the initial stage, the oxidation process occurred at the surface active sites including caps and defects of MWCNTs, which were of high electron density, thus preferentially reacted with ozone[18]. Later, caps and walls comprising a large amount of structural defects were etched by ozone molecules, which were triggered by the

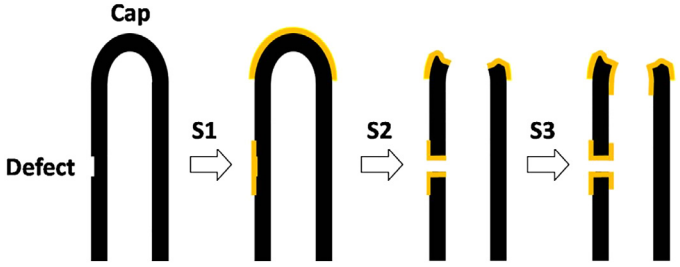

Scheme 1. Schematic process of the ozone-mediated functionalization of MWCNTs, in which the yellow location represents the formed oxygen functionalities.

functionalization at the first stage. Simultaneously, more carbon atoms exposed to ozone and functionalized by active oxygen atoms, significantly enhancing the oxygen contents especially the surf-O. The opened tips and penetrated walls of MWCNTs could also facilitate the inner surface to be accessible to ozone. As a result, the functionalization on the inner surface was prevailing at the third stage, which was evidenced by the difference between surf-O and over-O contents. Since the oxygen species on the inner surface were difficult to be detected by XPS, the obtained surf-O content did not increase like that of over-O. Inversely, due to the deeper oxidation of MWCNTs surfaces by ozone, some oxygen functionalities were oxidized into CO_2, leading to a decreased surf-O content (Fig. 4(a)) after 5 h. Another fact was that the etching at the second stage proceeded along the radial direction rather than the axial one, because the formed destructive zones were apt to suppress the reactivity of the adjacent atoms on the surface and thus prevented them burning off[10].

Our previous work[19] has proposed that the carboxylic groups on MWCNTs played a pivotal role in the electrocatalytic ORR reaction. So we employed this reaction as a probe reaction to investigate the catalytic properties of O_3-mediated functionalized MWCNTs by the cyclic voltammetry (CV) method in 0.1 mol/L KOH solution that was saturated with N_2 or O_2. Under N_2 sweeping (Fig. 5(a)), the functionalized MWCNTs after treated for 9 h displayed a significantly increased CV area, indicating that the functionalization efficiently improved the capacitance of MWCNTs. The featureless CV curves of samples suggested the absence of metal impurities on the MWCNTs surface[20]. After switching the sweep gas, a notable signal peak attributed to ORR was observed in Fig. 5(b). The ORR onset potential was determined from the intersection of the two tangents drown at the rising current and the background current density of the CV curves[21], while the ORR activity was defined as the absolute current density obtained by subtracting the corresponding background value from the peak value. The functionalized MWCNTs displayed a clear ORR peak potential at –0.252 V vs Ag/AgCl with –1.772 mA cm^{-2} of current density, while the pristine MWCNTs exhibited a more negative peak potential at –0.356 V vs Ag/AgCl with the current density at –1.193 mA cm^{-2}. Such an outstanding performance is comparable to or even higher than those of some nitrogen and phosphorus doped carbon materials[22,23]. The CV tests in O_2 saturated electrolyte verified that the O_3-mediated functionalization played an important role in enhancing the ORR activity of MWCNTs, which was further evidenced by the correlation of CV onset and peak potentials with the concentrations of oxygen functionalities. The linear regression analysis was performed for the structure–activity relationship between ORR potentials and the concentration of carboxyl, phenolic hydroxyl as well as lactone. As a result, only the carboxyl showed a much closer correlation with ORR potentials than the other oxygen-containing groups. Fig. 5(c) revealed a direct decline in the ORR over-potentials (the absolute values of CV onset and peak potentials) with the increasing concentration of carboxyl, which matched very well with our previous investigation[19]. Nonetheless, the ORR current density appeared a distinct different trend with the increasing concentration

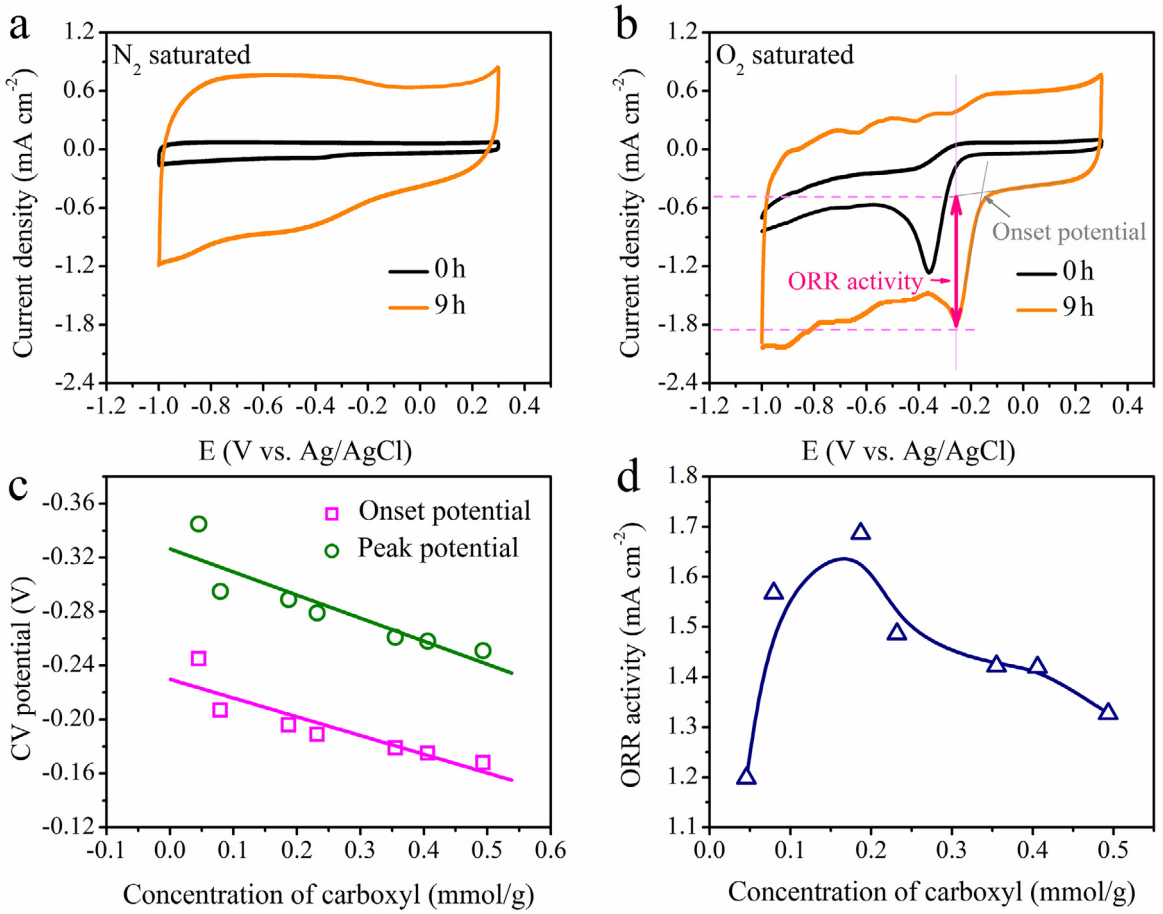

Fig. 5. CV curves saturated with N_2 (a) and O_2 (b) of pristine MWCNTs (black) and MWCNTs functionalized for 9 h (yellow); (c) Linear regression analysis between ORR potentials and concentration of carboxyl; (d) ORR activity as a function of concentration of carboxyl. The onset potential and the ORR activity were calculated as shown in Fig. 5(b).

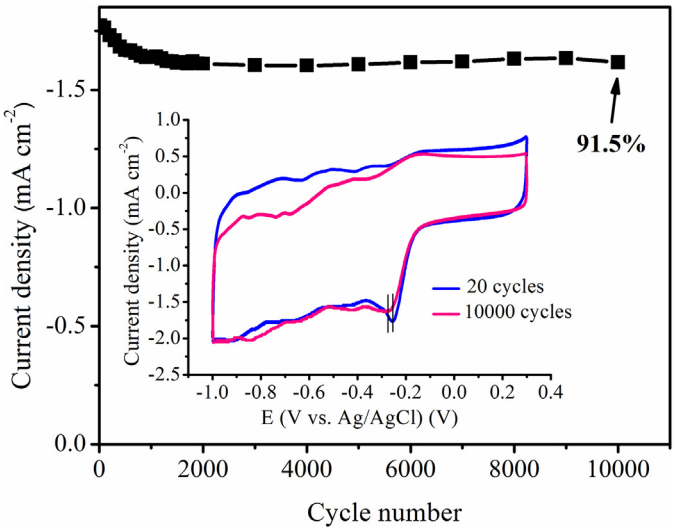

Fig. 6. Peak current density of functionalized MWCNTs (9 h) recorded during repeated cycling in oxygen saturated 0.1 mol/L KOH solution. The inset shows CV curves in different cycles.

of carboxyl. As seen in Fig. 5(d), the O_3 treatment overall improved the catalytic activity of MWCNTs with a higher ORR current density than the pristine sample. It could be explained that the attack of O_3 resulted in a carboxyl modified carbon surface and more defective graphitic structure to active oxygen molecules. Additionally, the exposed oxygen functionalities enhanced the hydrophilicity of MWCNTs, which strengthened the affinity between electrolyte and oxygen, and consequential oxygen diffusion to the catalyst surface[24]. Wu et al.[25] confirmed that the presence of surface oxygen groups was necessary for the ORR activity rather than the edge defects in sp^3 configuration. Tian et al.[26] also proposed the fully exposed active sites can effectively catalyze the oxygen reduction and evolution reaction. However, the modification of oxygen-containing groups and O_3 etching to graphitic lattice gave rise to an obvious reduction of electrical conductivity of MWCNTs, or a more difficult electron transport in carbon frameworks[27]. It was therefore well understood that the most active catalyst was the O_3-modified MWCNTs treated at 1 h with moderate carboxylic concentration of 0.2 mmol g^{-1}. We further checked the ORR durability of the functionalized MWCNTs catalyst (9 h) in oxygen saturated 0.1 mol/L KOH solution at the scanning rate of 100 mV s^{-1} (Fig. 6). The catalyst exhibited a slight declined activity with a current retention of 91.5% even after 10 000 cycles (about 71.5 h). Simultaneously, the inserted CV curves in Fig. 6 show a tiny negative shift of potential from –0.252 V vs Ag/AgCl to –0.275 V vs Ag/AgCl. Given all the above electrochemical analysis, the O_3 treatment predicts a promising method to achieve active and stable carbon materials for ORR application.

4. Conclusion

The O_3-mediated functionalization mechanism of MWCNTs and the catalytic performance of functionalized MWCNTs in the ORR reaction were systematically investigated. The interaction process probably undergoes three stages, which comprises the functionalization of carbons at the surface sites like caps and defects, further etching of curved caps and defective walls by O_3 to open tips and penetrate walls, and the functionalization of the inner and fractured surfaces. The phenolic hydroxyl was initially formed and then gradually oxidized into carboxyl as well as lactone. The carboxyl was found to play a pivotal role to reduce the ORR overpotentials and therefore improve the electrocatalytic activity of MWCNTs. However, the excess amount of oxygen-containing groups would obstruct the electron transport and consequently perform low current densities. The ORR activity of MWCNTs can be dramatically improved by realizing an appropriate functionalization extent and a prevailing fraction of carboxyl.

Acknowledgments

This work was financially supported by the National Natural Science Foundation of China (Nos. 21307142 and 21403261) and Ningbo Science and Technology Bureau (No. 2014D10004).

References

[1] D.S. Su, J. Zhang, B. Frank, A. Thomas, X. Wang, J. Paraknowitsch, R. Schlögl, ChemSusChem 3 (2010) 169–180.
[2] L.B. Chu, X.H. Xing, A.F. Yu, X.L. Sun, B. Jurcik, Process Saf. Environ. Prot. 86 (2008) 389–393.
[3] J. Zhang, X. Liu, R. Blume, A. Zhang, R. Schlögl, D.S. Su, Science 322 (2008) 73–77.
[4] J. Zhang, H. Zou, Q. Qing, Y. Yang, Q. Li, Z. Liu, X. Guo, Z. Du, J. Phys. Chem. B 107 (2003) 3712–3718.
[5] A. Barinov, L. Gregoratti, P. Dudin, S. La Rosa, M. Kiskinova, Adv. Mater. 21 (2009) 1916–1920.
[6] A.I. Aria, M. Gharib, Langmuir 27 (2011) 9005–9011.
[7] M. Li, M. Boggs, T.P. Beebe, C.P. Huang, Carbon 46 (2008) 466–475.
[8] X. Lu, F. Tian, X. Xu, N. Wang, Q. Zhang, J. Am. Chem. Soc. 125 (2003) 10459–10464.
[9] S.B. Hočevar, J. Wang, R.P. Deo, M. Musameh, B. Ogorevc, Electroanalysis 17 (2005) 417–422.
[10] S.D. Razumovskii, V.N. Gorshenev, A.L. Kovarskii, A.M. Kuznetsov, A.N. Shchegolikhin, Fuller. Nanotub. Carbon Nanostruct. 15 (2007) 53–63.
[11] H.L. Chiang, C.P. Huang, P.C. Chiang, Chemosphere 47 (2002) 257–265.
[12] D.C. Vennerberg, R.L. Quirino, Y. Jang, M.R. Kessler, ACS Appl. Mater. Interfaces 6 (2014) 1835–1842.
[13] X.L. Luo, J.J. Xu, J.L. Wang, H.Y. Chen, Chem. Commun. 16 (2005) 2169–2171.
[14] H. Huang, C.H. Liu, Y. Wu, S. Fan, Adv. Mater. 17 (2005) 1652–1656.
[15] D.J. Li, U.N. Maiti, J. Lim, D.S. Choi, W.J. Lee, Y. Oh, G.Y. Lee, S.O. Kim, Nano Lett. 14 (2014) 1228–1233.
[16] V.N. Khabashesku, W.E. Billups, J.L. Margrave, Acc. Chem. Res. 35 (2002) 1087–1095.
[17] C.T. Hsieh, H. Teng, W.Y. Chen, Y.S. Cheng, Carbon 48 (2010) 4219–4229.
[18] J.M. Lee, J.S. Park, S.H. Lee, H. Kim, S. Yoo, S.O. Kim, Adv. Mater. 23 (2011) 629–633.
[19] Y. Zhang, C. Chen, L. Peng, Z. Ma, Y. Zhang, H. Xia, A. Yang, L. Wang, D. Su, J. Zhang, Nano Res. 8 (2015) 502–511.
[20] K. Gong, F. Du, Z. Xia, M. Durstock, L. Dai, Science 323 (2009) 760–764.
[21] C.W. Liu, C.M. Lai, J.N. Lin, L.D. Tsai, K.W. Wang, RSC Adv. 4 (2014) 15820–15824.
[22] R. Liu, D. Wu, X. Feng, K. Müllen, Angew. Chem. 122 (2010) 2619–2623.
[23] Z.W. Liu, F. Peng, H.J. Wang, H. Yu, W.X. Zheng, J. Yang, Angew. Chem. 50 (2011) 3257–3261.
[24] I.Y. Jeon, H.J. Choi, S.M. Jung, J.M. Seo, M.J. Kim, L. Dai, J.B. Baek, J. Am. Chem. Soc. 135 (2012) 1386–1393.
[25] K.H. Wu, D.W. Wang, I.R. Gentle, Carbon 81 (2015) 295–304.
[26] G.L. Tian, Q. Zhang, B. Zhang, Y.G. Jin, J.Q. Huang, D.S. Su, F. Wei, Adv. Funct. Mater. 24 (2014) 5956–5961.
[27] Y.J. Kim, T.S. Shin, H.D. Choi, J.H. Kwon, Y.C. Chung, H.G. Yoon, Carbon 43 (2005) 23–30.